PERGAMON International Journal of Non-Linear Mechanics 37 (2002) 43–73

INTERNATIONAL JOURNAL OF
NON-LINEAR
MECHANICS

www.elsevier.com/locate/ijnonlinmec

Subharmonic resonance in the non-linear Mathieu equation

Randolph S. Zounes[a,*], Richard H. Rand[b]

[a]*Center for Applied Mathematics (CAM), Cornell University, Ithaca, NY 14853, USA*
[b]*Department of Theoretical and Applied Mechanics (T&AM), Cornell University, Ithaca, NY 14853, USA*

Received 29 November 1999

Abstract

In this paper, we present an $\mathcal{O}(\varepsilon)$ perturbation method that utilizes Lie transform perturbation theory and elliptic functions to investigate subharmonic resonances in the non-linear Mathieu equation

$$\ddot{x} + (\delta + \varepsilon\cos\omega t)x + \alpha x^3 = 0.$$

It is assumed that the parametric perturbation, $\varepsilon\cos\omega t$, is small and that the coefficient of the non-linear term, α, is positive but not necessarily small. We derive analytic expressions for features (width and location of equilibria) of resonance bands in a Poincaré section of action-angle space that are associated with $2m:1$ subharmonic periodic solutions. In contrast to previous perturbation treatments of this problem, the unperturbed system is non-linear and the transformation to action-angle variables involves elliptic functions. We are, therefore, not restricted to a neighborhood of the origin in our investigation.

The Hamiltonian structure of the unperturbed vector field, an *integrable* vector field, provides us with a framework for developing an analysis of the perturbed orbit structure. The methodolgy revolves around employing Lie transform perturbation theory for constructing the so-called "resonance Kamiltonian", K_r, whose level curves correspond to invariant curves of a Poincaré map for the non-linear Mathieu equation. Explicit knowledge of K_r enables us to derive analytic expressions for the resonance bands in a Poincaré section of action-angle space that are associated with $2m:1$ subharmonic periodic solutions. Predictions of the perturbation method are compared to results obtained by direct numerical integration of the non-linear Mathieu equation.

The integrable nature of the unperturbed ($\varepsilon = 0$) non-linear Mathieu equation is preserved under the perturbation method. Consequently, the method is unable to predict the appearance of chaos. © 2001 Published by Elsevier Science Ltd.

1. Introduction

In this paper, we employ Lie transform perturbation theory to investigate the nature of non-linear resonances in the non-linear Mathieu equation

$$\ddot{x} + (\delta + \varepsilon\cos\omega t)x + \alpha x^3 = 0. \tag{1.1}$$

* Corresponding author.
E-mail addresses: zounes@cam.cornell.edu (R.S. Zounes), rhr2@cornell.edu (R.H. Rand).

0020-7462/01/$ - see front matter © 2001 Published by Elsevier Science Ltd.
PII: S0020-7462(00)00095-0

We assume that the parametric perturbation, $\varepsilon \cos \omega t$, is small and that the coefficient of the non-linear term, α, is positive but not necessarily small. We derive analytic expressions for features (width and location of equilibria) of resonance bands in a Poincaré section of action-angle space that are associated with $2m:1$ subharmonic periodic solutions of Eq. (1.1). In contrast to previous perturbation treatments of this problem (e.g. [1,2]), the unperturbed system is non-linear and the transformation $(x, y) \to (\Phi, J)$ to action-angle variables involves elliptic functions. Consequently, we are not restricted to a neighborhood of the origin in our investigation.

It is well known that a small parametric excitation in the *linear* Mathieu equation ($\alpha = 0$) can produce unbounded motion when the frequency of the parametric forcing, ω, is about double the natural frequency of the system. Such an occurrence is referred to as a *primary parametric resonance* [2] and is associated with $2:1$ subharmonic periodic motions; i.e. $2\Omega = \omega$, where Ω is the natural frequency of the unperturbed system. Secondary resonances are also present and are associated with harmonic and $2:n$ superharmonic motions: $\Omega = \omega$ and $2\Omega_n = n\omega$, $n > 2$, respectively.

When a non-linearity is introduced ($\alpha \neq 0$), the response of the system is much more complicated [3]. There can be harmonic motions as well as an infinity of $2m:1$ subharmonic motions,

$$2m\Omega_m = \omega, \quad m = 1, 2, 3, \ldots,$$

an infinity of $2:n$ superharmonic motions,

$$2\Omega_n = n\omega, \quad n = 3, 4, 5, \ldots,$$

or in general, a double-infinity of $2m:n$ supersubharmonic motions,

$$2m\Omega_{mn} = n\omega, \quad n, m = 1, 2, 3, \ldots .$$

Although the latter relation suggests that the set of resonances $\{\Omega_{mn}\}$ is dense, this paper examines the $2m:1$ subharmonics and corresponding resonance bands, the only harmonics "visible" at the $\mathcal{O}(\varepsilon)$ level of analysis. In general, resonance bands associated with $2:1$ and $4:1$ subharmonic periodic motions are of primary interest since higher-order bands occupy significantly smaller regions of phase space.

Obtaining an approximate Poincaré map to study the nature of orbits near a resonance band constitutes a significant component of this paper and is accomplished in a series of steps. We first make use of the Hamiltonian structure of the unperturbed vector field, an *integrable* vector field, to provide us with a framework for developing an analysis of the perturbed orbit structure. Then, utilizing Lie transform perturbation theory, the non-autonomous Hamiltonian induced by

$$\begin{aligned} \dot{x} &= y, \\ \dot{y} &= -(\delta + \varepsilon \cos \omega t)\, x - \alpha x^3, \end{aligned} \tag{1.2}$$

a system equivalent to Eq. (1.1), is reduced to an autonomous one by means of a periodic, near-identity transformation. The resulting autonomous Hamiltonian delivers an approximate Poincaré map of the perturbed system whereby level curves of the transformed Hamiltonian correspond to invariant curves of the Poincaré map.

An important feature of the proceeding analysis is its underlying dependence on Kolmogorov–Arnold–Moser (KAM) theory and Moser's Twist Theorem for providing qualitative features of Poincaré maps for Eq. (1.2). Roughly speaking, when an N-degree-of-freedom integrable Hamiltonian system is made slightly non-integrable with the introduction of a Hamiltonian perturbation, the "sufficiently irrational" orbits of the vector field remain confined to invariant N-tori (KAM surfaces); i.e. most N-tori survive the perturbation. Or if seen in plane sections, most of the invariant closed curves of the unperturbed system

continue to exist. We shall examine the remnants of those tori associated with $2m:1$ subharmonic periodic orbits of the non-linear Mathieu equation that do not survive the introduction of the perturbation. A detailed exposition on the non-linear Mathieu equation and related topics is given in [4].

2. Preliminaries: action-angle space, Poincaré maps, and rudiments of KAM theory

The non-autonomous Hamiltonian induced by (1.2) may be written

$$H(x,y,t) = \tfrac{1}{2}y^2 + \tfrac{1}{2}x^2(\delta + \varepsilon\cos\omega t) + \tfrac{1}{4}\alpha x^4, \tag{2.1}$$

where x and y are canonically conjugate variables. Since the unperturbed system ($\varepsilon = 0$) is integrable, there exists a canonical transformation into action-angle variables $(x,y) \to (\Phi, J)$ under which the transformed, unperturbed Hamiltonian takes the form

$$H = H_0(J).$$

The unperturbed vector field becomes

$$\dot{J} = -\frac{\partial H_0}{\partial \Phi} = 0,$$

$$\dot{\Phi} = \frac{\partial H_0}{\partial J} \equiv \Omega(J),$$

hence, J is constant on unperturbed orbits and specifying J specifies an orbit. Since $\alpha > 0$, all solutions are periodic with period $T(J) = 2\pi/\Omega(J)$ and form closed curves around the origin. Note that for small J, $\Omega(J) \sim \sqrt{\delta}$, the natural frequency of the unperturbed, linear system.

Extending phase space and transforming the coordinates of the perturbed vector field to action-angle coordinates (see Section 1.2 of [3]), the perturbed vector field takes the form

$$\begin{aligned} \dot{J} &= \varepsilon F_1(J,\Phi,\theta), \\ \dot{\Phi} &= \Omega(J) + \varepsilon F_2(J,\Phi,\theta), \quad (J,\Phi,\theta) \in \mathbb{R}^+ \times T^2, \\ \dot{\theta} &= \omega, \end{aligned} \tag{2.2}$$

for some functions F_1 and F_2 both of which are 2π periodic in Φ and θ. Next, take a global cross-section to the flow,

$$\Sigma = \{(J,\Phi,\theta):\ \theta = \theta_0 \in [0, 2\pi)\},$$

and consider the Poincaré map $P_\varepsilon: \Sigma \to \Sigma$ induced by solutions of (2.2). When $\varepsilon = 0$, the map is simply the time-$2\pi/\omega$ flow map of the unperturbed system:

$$P_0: (J,\Phi) \mapsto (J,\ \Phi + 2\pi\Omega(J)/\omega).$$

When transformed back to (x,y) coordinates, all orbits lie on closed, invariant curves, and the quantity $2\pi\Omega(J)/\omega$ dictates the extent to which points rotate per iteration. The orbit is dense if $\Omega(J)/\omega$ is irrational, and orbits of P_0 will appear to coincide with the level curves of the unperturbed Hamiltonian. In addition, since $\Omega(J)$ increases with J,[1] the average angle turned by points under P_0 increases as one moves out across the invariant curves. Therefore, P_0 is referred to as a *twist mapping*.

[1] We show later that $\Omega'(J) > 0$ for $J \geqslant 0$.

Of particular interest to us are the $2m:1$ subharmonics, orbits whose frequencies are related to the frequency of the parametric forcing through the *resonance relation*,

$$\omega = 2m\Omega(J), \quad m \in \mathbb{Z}^+.$$

A "resonant periodic orbit" is an orbit whose frequency satisfies the resonance relation, and it will be referred to (loosely) as a "resonant torus". We speak of the "resonance band" emerging from a resonant torus as the region of the Poincaré cross-section near an action value J_m that satisfies the resonance relation; i.e. a neighborhood of $J = J_m$ for which $\omega = 2m\Omega(J_m)$, for some $m \in \mathbb{Z}^+$.

The KAM Theorem and Moser's Twist Theorem allow us to utilize the global geometry of the unperturbed phase space for determining qualitative features of the perturbed Poincaré map,

$$P_\varepsilon : (J, \Phi) \mapsto (J + \varepsilon f_1(J, \Phi),\ \Phi + 2\pi\Omega(J)/\omega + \varepsilon f_2(J, \Phi)),$$

for some functions f_1 and f_2, seen as a perturbation of P_0. As discussed above, the theorems assert that the non-resonant invariant curves of P_0 — those curves having the property that $\Omega(J)/\omega$ is sufficiently irrational in a number-theoretic sense — are preserved for P_ε if ε is sufficiently small. The theorems allow us to focus solely on the resonant tori in our analysis of the non-linear Mathieu equation. For completeness, modified versions of both theorems, as given in [5,6], are stated in the context of the present system.

Theorem 2.1 (KAM). *Suppose $\Omega'(J) \neq 0$ for $J \geqslant 0$. Then "most" of the invariant closed curves in P_0 persist for sufficiently small ε. The motion on the associated tori of these surviving curves is quasiperiodic, having $m = 2$ rationally incommensurate frequencies. These invariant closed curves form a majority in the sense that the Lebesgue measure of the complement of their union is small when ε is small.*

Moser's Twist Theorem is more specific and applicable for our needs:

Theorem 2.2 (Twist). *Assume $\Omega(J)$ is C^r, $r \geqslant 5$, and $|\Omega'(J)| \geqslant \nu > 0$ on an annulus $R = \{(J, \Phi)\colon J_1 \leqslant J \leqslant J_2\}$. Then there exists a δ depending on both ε and $\Omega(J)$ such that, if the perturbed map P_ε satisfies*[2]

$$\sup_{(J,\Phi)\in R} \varepsilon[\|f_1\|_r + \|f_2\|_r] < \nu\delta,$$

then P_ε possesses an invariant curve Γ_ε in R of the form

$$J = J_m + U(\psi), \qquad \Phi = \psi + V(\psi),$$

where U and V are C^1, of period 2π,

$$\|U\|_1 + \|V\|_1 < \varepsilon$$

and $J_1 < J_m < J_2$. Moreover, the map restricted to this invariant curve is given by

$$\Phi \mapsto \Phi + 2\pi\frac{\lambda}{\omega}, \quad \Phi \in [0, 2\pi),$$

where λ/ω is irrational and satisfies the infinite set of relations

$$\left|\frac{\lambda}{\omega} - \frac{n}{m}\right| \geqslant \gamma m^{-\alpha} \tag{2.3}$$

[2] $\|F\|_r$ denotes the C^r norm $\sum_{k=0}^{r} |D^k F(J, \Phi)|$.

for some $\gamma, \alpha > 0$ *and all integers* $m, n > 0$. *Each choice of* $\lambda \in [\Omega(J_1), \Omega(J_2)]$ *satisfying* (2.3) *gives rise to such an invariant curve.*

An important requisite for the application of the two theorems is that $\Omega'(J) \neq 0$; i.e. the dependence of the frequency of oscillation on amplitude or energy. From a mechanical point of view, motion under non-linear resonance is prevented from becoming unbounded: as the amplitude of motion increases, the frequency increases,[3] and the system ceases to be in resonance. From a dynamical systems point of view, the existence of invariant curves prevents unbounded motion: persisting 2-tori associated with the invariant curves of P_ε provide boundaries in the three-dimensional energy manifold across which trajectories cannot pass. Hence, trajectories of the perturbed vector field either remain on invariant 2-tori not destroyed under the perturbation, or evolve in the phase space between pairs of such tori (the plane sections of which are the resonance bands).

3. Unperturbed system and construction of action-angle variables

In this section, we derive the general solution to the unperturbed ($\varepsilon = 0$) non-linear Mathieu equation

$$\ddot{f} + \delta f + \alpha f^3 = 0, \tag{3.1}$$

which can be viewed as the equation of motion for a particle of unit mass confined to a quartic well. It is assumed, as stated above, that $\alpha > 0$; we make the additional assumption that $\delta > 0$. We shall see that for all parameter values, solutions of Eq. (3.1) are periodic and can be expressed in terms of Jacobi elliptic functions. Our goal is to use a solution of (3.1) to construct action-angle variables to which the perturbed system ($\varepsilon \neq 0$) will be transformed. The reader may choose to skip to the end of this section for the equations defining the transformation $(x, y) \to (\Phi, J)$ to action-angle variables.

Before proceeding, it is advantageous first to scale time and space. By setting $\tau = \sqrt{\delta}t$ and $x = \sqrt{\alpha/\delta}f$, Eq. (3.1) is transformed into

$$x'' + x + x^3 = 0, \tag{3.2}$$

where the prime denotes differentiation with respect to τ. The original solution is extracted from the transformed one via the relation, $f(t) = \sqrt{\delta/\alpha}x(\sqrt{\delta}t)$.

The Hamiltonian induced by (3.2) may be written

$$H_0(x, y) = \tfrac{1}{2}y^2 + \tfrac{1}{2}x^2 + \tfrac{1}{4}x^4, \tag{3.3}$$

where x and y are canonically conjugate variables. If the system has total energy $h \geqslant 0$, then the "energy equation"

$$H_0(x, y) = \tfrac{1}{2}y^2 + \tfrac{1}{2}x^2 + \tfrac{1}{4}x^4 = h \tag{3.4}$$

determines the dynamics of a particle with kinetic energy $\frac{1}{2}y^2$ and potential energy $V(x) = \frac{1}{2}x^2 + \frac{1}{4}x^4$ moving harmonically between turning points, $x = \pm X_t$. The turning points (or amplitude) are defined via the relation $V(\pm X_t) = h$, which corresponds to the instant when the total energy of the system is completely potential (see Fig. 1). Specifically, the turning points satisfy the equation $h = \frac{1}{2}X_t^2 + \frac{1}{4}X_t^4$, or inverting, $X_t^2 = \sqrt{1 + 4h} - 1$.

[3] The fact that the frequency of oscillation increases as the energy is increased is a direct consequence of our assumption that $\alpha > 0$.

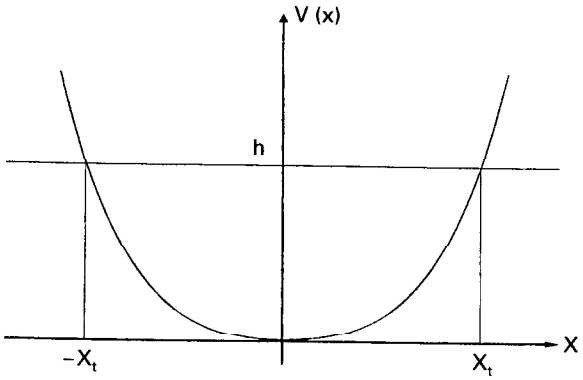

Fig. 1. Potential energy $V(x) = \frac{1}{2}x^2 + \frac{1}{4}x^4$ of Hamiltonian. A particle with total energy h moves harmonically between the turning points, $\pm X_t$.

The general solution of Eq. (3.2) is readily obtained by manipulating the energy equation, (3.4). Solving for $y = \mathrm{d}x/\mathrm{d}\tau$ and separating variables yields

$$\mathrm{d}\tau = \frac{\mathrm{d}x}{\sqrt{2h - x^2 - \frac{1}{2}x^4}}. \tag{3.5}$$

We remark that of the two possible roots " + " or " − " arising from solving (3.4) for y, the " − " root is extraneous. We keep the " + " root because this implies that $\mathrm{d}y/\mathrm{d}x = \dot{y}/\dot{x} < 0$ for $x > 0$; i.e. motion in phase space is clockwise.

By expressing h in terms of X_t, defining $W = x/X_t$, rearranging, and integrating, Eq. (3.5) is rewritten in the form

$$u_0 + \sqrt{1 + X_t^2}\int_0^\tau \mathrm{d}\tau = \int_0^{x/X_t} \frac{\mathrm{d}W}{\sqrt{(1 - W^2)((1 - k^2) + k^2W^2)}}, \tag{3.6}$$

where the *elliptic modulus* k is defined by

$$k^2 \overset{\text{def}}{=} \frac{X_t^2}{2(1 + X_t^2)}, \tag{3.7}$$

the phase u_0 is given by

$$u_0 = \int_0^{x_0/X_t} \frac{\mathrm{d}W}{\sqrt{(1 - W^2)((1 - k^2) + k^2W^2)}} \tag{3.8}$$

and x_0 is the initial position of the particle, $x_0 = x(\tau - 0)$. The above integral (3.6) is recognized as being the inverse elliptic function, $\mathrm{cn}^{-1}(x/X_t, k)$. Hence, we find that the general solution of Eq. (3.2) is

$$x(\tau) = X_t\ \mathrm{cn}(u_0 \mid \sqrt{1 + X_t^2}\tau, k), \tag{3.9}$$

$$y(\tau) = x'(\tau)$$

$$= -X_t\sqrt{1 + X_t^2}\,\mathrm{sn}(u_0 + \sqrt{1 + X_t^2}\tau, k)\mathrm{dn}(u_0 + \sqrt{1 + X_t^2}\tau, k). \tag{3.10}$$

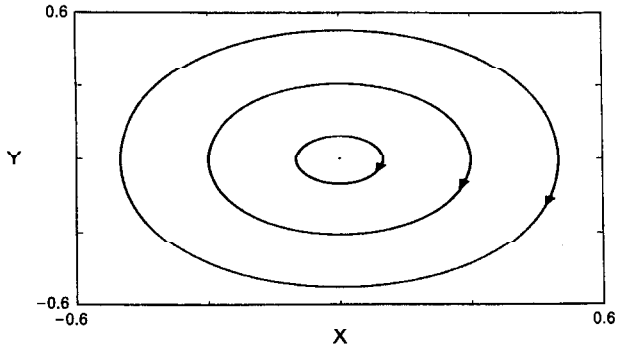

Fig. 2. Phase space of the unperturbed ($\varepsilon = 0$) non-linear Mathieu system (3.2). Space and time have been scaled.

The particular solution of (3.2) with initial conditions $x(0) = X_t$, $y(0) = 0$ is then

$$x(\tau) = X_t \operatorname{cn}(\sqrt{1 + X_t^2}\tau, k),$$
$$y(\tau) = -X_t\sqrt{1 + X_t^2}\operatorname{sn}(\sqrt{1 + X_t^2}\tau, k)\operatorname{dn}(\sqrt{1 + X_t^2}\tau, k). \tag{3.11}$$

A sketch of the phase space for this system is given in Fig. 2. We see that the phase space contains a single elliptic fixed point at the origin surrounded by a one-parameter family of periodic orbits indexed by k. Since the period in u of the elliptic function $\operatorname{cn}(u, k)$ is $4K(k)$, $K(k)$ being the *complete elliptic integral of the first kind*, the period in τ of a particular orbit (specified by k) is

$$T(k) = \oint \mathrm{d}\tau = \oint \frac{1}{\mathrm{d}u/\mathrm{d}\tau}\mathrm{d}u = \frac{4K(k)}{\sqrt{1 + X_t^2}} \tag{3.12}$$

and the corrresponding natural frequency of the system is

$$\Omega(k) = \frac{2\pi}{T(k)} = \frac{\pi\sqrt{1 + X_t^2}}{2K(k)}. \tag{3.13}$$

The reader is reminded that specifying k is equivalent to specifying h or specifying X_t. In particular, the inversion of Eq. (3.7) yields the relation

$$X_t^2 = \frac{2k^2}{1 - 2k^2}. \tag{3.14}$$

Note that the frequency of oscillation increases as the energy of the system is increased, which is due to our assumption that $\alpha > 0$. This is more in line with elastic systems as opposed to pendulum sytems in which the opposite effect is observed.

We are now in a position to define action-angle variables (Φ, J). These permit the unperturbed Hamiltonian to be written in a simplified form while still retaining the Hamiltonian form of the governing equations. Consider the periodic orbit, Γ_h, defined by the energy equation, $H_0(x, y) = h$. As illustrated in Fig. 2, the area enclosed by Γ_h in phase space is constant in time. We define, therefore, the action associated with Γ_h as this area, divided by the normalization factor 2π:

$$J = \frac{1}{2\pi}\oint_{\Gamma_h} y\,\mathrm{d}x. \tag{3.15}$$

Expressing as an integral in τ,

$$J = \frac{1}{2\pi}\int_0^{T(k)} [y(\tau)]^2 \, d\tau,$$

substituting in Eqs. (3.11) and (3.12), and integrating, we obtain

$$J = \frac{4}{3\pi}\sqrt{1 + X_t^2}\left(- E(k) + \left(1 + \frac{1}{2}X_t^2\right)K(k)\right), \tag{3.16}$$

where $E(k)$ is the *complete elliptic integral of the second kind*. Since $k = k(X_t)$ and $X_t = X_t(h)$, J may be seen as a function of h and inverting [4] gives h as a function of J: $H_0 = h(J)$. Similarly, J may be seen as a function of X_t and inverting yields X_t as a function of J: $X_t = X_t(J)$. By employing Hamilton's equations, we find that

$$\frac{dJ}{d\tau} = -\frac{\partial h}{\partial \Phi} = 0$$

and as defined, J remains constant in time along a trajectory. The angle-variable Φ is chosen so that the transformation $(x, y) \to (\Phi, J)$ is canonical:

$$\frac{d\Phi}{d\tau} = \frac{\partial h}{\partial J} = \frac{dh/dX_t}{dJ/dX_t} = \frac{\pi\sqrt{1 + X_t^2}}{2K(k)} = \Omega(k) \tag{3.17}$$

implying that

$$\Phi = \Phi(0) + \Omega(k)\tau.$$

If we make the replacement $\tau \to \Phi/\Omega(k)$ in Eqs. (3.11), we obtain the following equations for the canonical transformation between (x, y) and (Φ, J):

$$x(J, \Phi) = X_t(J)\,\mathrm{cn}\left(4K(k)\frac{\Phi}{2\pi}, k\right), \tag{3.18}$$

$$y(J, \Phi) = -X_t(J)\sqrt{1 + X_t^2}\,\mathrm{sn}\left(4K(k)\frac{\Phi}{2\pi}, k\right)\mathrm{dn}\left(4K(k)\frac{\Phi}{2\pi}, k\right), \tag{3.19}$$

where it is understood that $k = k(J)$.

4. Transformation of non-autonomous Hamiltonian for application of Lie transforms

The principal objective of this paper is to derive analytic expressions for the width of and location of equilibria within resonance bands in a Poincaré section of action-angle space that are associated with $2m:1$ subharmonic periodic solutions of the non-linear Mathieu equation (1.1). The methodolgy revolves around employing Lie transform perturbation theory for constructing the so-called "resonance Kamiltonian", K_r, whose level curves correspond to invariant curves of the Poincaré map. The purpose of this section is to transform the non-autonomous Hamiltonian (2.1), induced by the non-linear Mathuieu equation, to a form for the direct application of Lie transforms.

[4] $J'(h) > 0$ for $h > 0$; cf. Eq. (3.17).

The Hamiltonian induced by the non-linear Mathieu equation, upon scaling time and space according to $\tau \to \sqrt{\delta}t$ and $x \to \sqrt{\alpha/\delta}x$, may be written as

$$H(x,y,\tau) = \frac{1}{2}y^2 + \frac{1}{2}x^2\left[1 + \frac{\varepsilon}{\delta}\cos\left(\frac{\omega}{\sqrt{\delta}}\tau\right)\right] + \frac{1}{4}x^4$$

$$= H_0(x,y) + \frac{\varepsilon}{2\delta}x^2\cos\left(\frac{\omega}{\sqrt{\delta}}\tau\right), \tag{4.1}$$

where x and y are canonically conjugate variables and $H_0(x,y) = \frac{1}{2}y^2 + \frac{1}{2}x^2 + \frac{1}{4}x^4$, as defined earlier in Eq. (3.3). In the action-angle coordinate system defined by Eqs. (3.16), (3.18), and (3.19), the canonically transformed Hamiltonian becomes

$$H(\Phi,J,\tau) = H_0(x(J,\Phi),y(J,\Phi)) + \frac{\varepsilon}{2\delta}x^2(J,\Phi)\cos\left(\frac{\omega}{\sqrt{\delta}}\tau\right)$$

$$= h(J) + \frac{\varepsilon}{2\delta}X_t^2(J)\,\mathrm{cn}^2\left(4K(k)\frac{\Phi}{2\pi},k\right)\cos\left(\frac{\omega}{\sqrt{\delta}}\tau\right), \tag{4.2}$$

where the unperturbed component of the Hamiltonian expressed in terms of the amplitude X_t is

$$h(J) = \tfrac{1}{2}X_t^2(J) + \tfrac{1}{4}X_t^4(J). \tag{4.3}$$

It is convenient to proceed first with the introduction of an additional canonical transformation $(\Phi,J) \to (\phi,j)$ before expanding the Hamiltonian (exposing those harmonics visible at the $\mathcal{O}(\varepsilon)$ level of analysis) and applying Lie transforms. The new momentum, j, also referred to as "action" because $J \sim j$ for small amplitudes, is defined by the relation

$$j(J) = \tfrac{1}{2}X_t^2(J). \tag{4.4}$$

The elliptic modulus, k, now viewed as a function of j satisfies

$$k^2 \overset{\text{def}}{=} \frac{\frac{1}{2}X_t^2}{1+X_t^2} = \frac{j}{1+2j} \tag{4.5}$$

and the action, J, expressed as a function of j becomes

$$J(j) = \frac{4}{3\pi}\sqrt{1+2j}(-E(k(j)) + (1+j)K(k(j)))$$

$$= \tfrac{2}{3}\sqrt{1}2j(-\tilde{E}(j) + (1+j)\tilde{K}(j)), \tag{4.6}$$

where $\tilde{E}(j) \equiv (2/\pi)E(k(j))$ and $\tilde{K}(j) \equiv (2/\pi)K(k(j))$ are the normalized, complete elliptic integrals as functions of j. Eq. (4.6) provides the first of two equations for the transformation between (Φ,J) and (ϕ,j). The second equation, $\Phi = \Phi(j,\phi)$, is constructed to make the transformation canonical; i.e. we need to find $\Phi(j,\phi)$ so that

$$\mathrm{d}J \wedge \mathrm{d}\Phi = \mathrm{d}j \wedge \mathrm{d}\phi.$$

Equivalently, $\Phi(j,\phi)$ is chosen to satisfy

$$J'(j)\frac{\partial\Phi}{\partial\phi} = 1,$$

where we used the fact that $\partial J/\partial\phi = 0$. Integrating with respect to ϕ yields the second equation of the canonical transformation:

$$\Phi(j,\phi) = \frac{\phi}{J'(j)}, \tag{4.7}$$

where

$$J'(j) = \frac{\mathrm{d}J}{\mathrm{d}j} = \sqrt{1+2j}\tilde{K}(j) = \frac{1+2j}{\Omega(j)}. \tag{4.8}$$

The natural frequency of the unperturbed system as a function of j, $\Omega(j)$, is found to be

$$\Omega(j) = \frac{\pi\sqrt{1+2j}}{2K(k(j))} = \frac{\sqrt{1+2j}}{\tilde{K}(j)} \tag{4.9}$$

and $J(j) \sim j$, $J'(j) \sim 1$, $\Omega(j) \sim 1$ for small j (as $j \to 0$).

In the new action-angle coordinate system defined by Eqs. (4.4), (4.6), and (4.7), the transformed Hamiltonian assumes the form

$$H(\phi,j,\tau) = H_0(j) + \varepsilon H_1(\phi,j,\tau), \tag{4.10}$$

where

$$H_0(j) = j + j^2, \tag{4.11}$$

$$\varepsilon H_1(\phi,j,\tau) = \frac{\varepsilon}{\delta} j \,\mathrm{cn}^2\left(\frac{\tilde{K}(j)}{J'(j)}\phi, k\right) \cos\left(\frac{\omega}{\sqrt{\delta}}\tau\right). \tag{4.12}$$

The efficacy of introducing the new action-angle coordinates is evident: we have a simple analytic expression for the Hamiltonian which, for small amplitudes of motion, is given in terms of the original action-angle variables.

We are now at a point in our analysis from which we can proceed only if the cn function is expanded in a Fourier series. One may question the original use of elliptic functions since we effectively replace them with trigonometric functions. There is, however, strong motivation for using elliptic functions and proceeding by expanding cn in a Fourier series:

1. As discussed above, no approximation to the unperturbed Hamiltonian has been made. Had trigonometric functions been used in the transformation $(x, y) \to (\Phi, J)$, higher-order harmonics of the unperturbed Hamiltonian would have been neglected, and $\mathcal{O}(\varepsilon^0)$ errors would then pervade the analysis. In particular, the frequency $\Omega = \partial H_0/\partial J$ of the system as a function of amplitude would not be known exactly, and consequently, the location of invariant tori (as defined by the resonance relation) would be approximate.
2. The expansion of cn in a Fourier series enables us to pick-up the $2m:1$ harmonics, even though our analysis is only $\mathcal{O}(\varepsilon)$. Had trigonometric functions been used, only the $2:1$ harmonic would be visible.

Continuing, expand the cn function in a Fourier series as given in Ref. [7] by Byrd and Friedman:

$$\mathrm{cn}(u,k) = \frac{2\pi}{kK}\sum_{n=0}^{\infty} g_n(k)\cos\left[(2n+1)\frac{\pi u}{2K}\right], \tag{4.13}$$

where

$$g_n(k) = \frac{1}{2}\mathrm{sech}\left[\left(n+\frac{1}{2}\right)\pi\frac{K'}{K}\right],$$

$K \equiv K(k)$, and $K' \equiv K(\sqrt{1-k^2})$. For the problem at hand, the expression for cn with arguments as given in Eq. (4.12) in the (ϕ, j) coordinate system becomes

$$\mathrm{cn}\left(\frac{\tilde{K}(j)}{J'(j)}\phi, k\right) = \sum_{n=0}^{\infty} G_n(j)\cos\left[(2n+1)\frac{\phi}{J'(j)}\right],$$

where the new coefficient, G_n, is defined by

$$G_n(j) = \frac{2\pi}{k(j)K(k(j))}g_n(k(j)) = \frac{4}{k(j)\tilde{K}(j)}g_n(k(j)). \tag{4.14}$$

Note that G_n decreases roughly exponentially with increasing n. Squaring the above expansion, reducing trigonometric terms, and collecting harmonics, we obtain our sought-after result:

$$\mathrm{cn}^2\left(\frac{\tilde{K}(j)}{J'(j)}\phi, k\right) - \mathscr{G}_0(j) + \sum_{m=1}^{\infty} \mathscr{G}_m(j)\cos\left(\frac{2m\phi}{J'(j)}\right), \tag{4.15}$$

where

$$\begin{aligned}
\mathscr{G}_0 &= \tfrac{1}{2}(G_0^2 + G_1^2 + G_2^2 + G_3^2 + \cdots) \sim \tfrac{1}{2} - \tfrac{1}{16}j + \tfrac{3}{32}j^2,\\
\mathscr{G}_1 &= \tfrac{1}{2}G_0^2 + G_0G_1 + G_1G_2 + G_2G_3 + \cdots \sim \tfrac{1}{2} - \tfrac{3}{512}j^2.\\
\mathscr{G}_2 &= G_0G_1 + G_0G_2 + G_1G_3 + G_2G_4 + \cdots \sim \tfrac{1}{16}j - \tfrac{3}{32}j^2.\\
&\vdots
\end{aligned}$$

Hence, the perturbed component of Hamiltonian (4.12) in the new action-angle coordinates (ϕj) is

$$\begin{aligned}
\varepsilon H_1(\phi, j, \tau) &= \frac{\varepsilon}{\delta} j\cos\left(\frac{\omega}{\sqrt{\delta}}\tau\right)\left[\mathscr{G}_0(j) + \sum_{m=1}^{\infty}\mathscr{G}_m(j)\cos\left(\frac{2m\phi}{J'(j)}\right)\right]\\
&= \frac{\varepsilon}{\delta} j\mathscr{G}_0(j)\cos\left(\frac{\omega}{\sqrt{\delta}}\tau\right) + \frac{\varepsilon}{2\delta} j\sum_{m=1}^{\infty}\mathscr{G}_m(j)\left[\cos\left(\frac{2m\phi}{J'(j)} + \frac{\omega}{\sqrt{\delta}}\tau\right) + \cos\left(\frac{2m\phi}{J'(j)} - \frac{\omega}{\sqrt{\delta}}\tau\right)\right],
\end{aligned} \tag{4.16}$$

in a form suitable for the direct application of Lie transform perturbation theory for reducing the non-autonomous Hamiltonian given by Eqs. (4.10), (4.11), and (4.16) to an autonomous one.

5. Application of Lie transforms to the non-linear Mathieu equation

The method of Lie transforms is a perturbation method for Hamiltonian systems that explicitly generates the functional form of the new Hamiltonian; explicit knowledge of the corresponding near-identity, canonical transformation is not required (see [8–10]). In contrast to other perturbation methods under which the vector field is perturbed, the method of Lie transforms perturbs only the Hamiltonian.

Let $(q, p) = (q_1, \ldots, q_n, p_1, \ldots, p_n)$ and $(Q, P) = (Q_1, \ldots, Q_n, P_1, \ldots, P_n)$ denote the old and new coordinates, respectively, and let H and K denote the respective Hamiltonians. The transformed Hamiltonian, K, not to be confused with the complete elliptic integral, is often called the "Kamiltonian" after Goldstein. The relation between (q, p) and (Q, P) is defined implicitly in terms of a Lie generating function $W(q, p, \tau; \varepsilon)$ as satisfying the conditions

$$\frac{\mathrm{d}q_i}{\mathrm{d}\varepsilon} = \frac{\partial W}{\partial p_i}, \quad \frac{\mathrm{d}p_i}{\mathrm{d}\varepsilon} = -\frac{\partial W}{\partial q_i} \tag{5.1}$$

and initial conditions

$$q_i(\varepsilon = 0) = Q_i, \quad p_i(\varepsilon = 0) = P_i \tag{5.2}$$

for $i = 1, 2, \ldots, n$. One can view this as a Hamiltonian system with Hamiltonian W and "time" ε that determines the evolution from the old coordinate system to the new coordinate system. W should not be confused with the global generating function of mixed variables, $F(q, P, \tau)$, used in Hamilton–Jacobi theory; W is a function of the old coordinates and specifies the transformation through the conditions given above, namely, (5.1) and (5.2).

Next, assume that the functions H, K, and W may each be written in a power series in ε:

$$H(q, p, \tau; \varepsilon) = H_0(q, p, \tau) + \varepsilon H_1(q, p, \tau) + \cdots, \tag{5.3}$$

$$K(Q, P, \tau; \varepsilon) = K_0(Q, P, \tau) + \varepsilon K_1(Q, P, \tau) + \cdots, \tag{5.4}$$

$$\begin{aligned} W(q, p, \tau; \varepsilon) &= W(q(Q, P), p(Q, P), \tau) \\ &= W_1(Q, P, \tau) + \varepsilon W_2(Q, P, \tau) + \cdots . \end{aligned} \tag{5.5}$$

Also expanding the explicit relations for the transformation $(q, p) \to (Q, P)$ each in a power series in ε,

$$q_i(Q, P, \tau; \varepsilon) = Q_i + \varepsilon q_i^1(Q, P, \tau) + \cdots,$$

$$p_i(Q, P, \tau; \varepsilon) = P_i + \varepsilon p_i^1(Q, P, \tau) + \cdots,$$

Eqs. (5.1) and (5.2) generate the following near-identity transformation [10]:

$$q_i = Q_i + \varepsilon \frac{\partial W_1}{\partial P_i} + \mathcal{O}(\varepsilon^2), \tag{5.6}$$

$$p_i = P_i - \varepsilon \frac{\partial W_1}{\partial Q_i} + \mathcal{O}(\varepsilon^2). \tag{5.7}$$

This transformation is canonical, and a proof may be found in the paper by Deprit [9]. Substituting (5.5)–(5.7) into expansion (5.3) of H and identifying terms with those in expansion (5.4) of K, we obtain the following relations between K and H:

$$K_0(Q, P, \tau) = H_0(Q, P, \tau), \tag{5.8}$$

$$K_1(Q, P, \tau) = H_1(Q, P, \tau) + \{H_0, W_1\} - \frac{\partial W_1}{\partial \tau},$$

$$\vdots \tag{5.9}$$

where $\{,\}$ is the Poisson bracket operator (or Lie derivative) defined by

$$\{f, g\} = \sum_{i=1}^{n} \frac{\partial f}{\partial Q_i}\frac{\partial g}{\partial P_i} - \frac{\partial f}{\partial P_i}\frac{\partial g}{\partial Q_i}. \tag{5.10}$$

The sequence (5.8), (5.9), ... of equations delivers the transformed Hamiltonian (Kamiltonian) for an arbitrary generating function, W. We can, therefore, choose successive W_i to make the corresponding K_i as simple as possible. Ideally, we would like to pick the generating function so that all higher-order terms of K vanish. However, this choice may lead to secular terms of small denominators in the transformation and the corresponding terms of the K_i must be kept. The strategy used for the non-linear Mathieu system, to be discussed next, is to restrict the analysis to a resonance band in phase space, thereby enabling us to transform away all but one of the infinitely many resonant terms in H_1.

We now apply the Lie transform perturbation method, outlined above, to simplify the Hamiltonian $H(\phi,j,\tau)$ defined by Eqs. (4.10), (4.11), and (4.16). The transformation from (ϕ,j) coordinates to (Q,P) coordinates is given by Eqs. (5.6) and (5.7):

$$\phi = Q + \varepsilon\frac{\partial W_1}{\partial P} + \mathcal{O}(\varepsilon^2),$$

$$j = P - \varepsilon\frac{\partial W_1}{\partial Q} + \mathcal{O}(\varepsilon^2).$$

In the new coordinates the transformed Hamiltonian (Kamiltonian), as defined by Eq. (5.4), becomes

$$K(Q,P,\tau) = K_0(P) + \varepsilon K_1(Q,P,\tau) + \mathcal{O}(\varepsilon^2), \tag{5.11}$$

where

$$\begin{aligned} K_0(P) &= H_0(Q,P,\tau) \\ &= P + P^2, \end{aligned} \tag{5.12}$$

$$\begin{aligned} K_1(Q,P,\tau) &= H_1(Q,P,\tau) + \{H_0, W_1\} - \frac{\partial W_1}{\partial \tau} \\ &= H_1(Q,P,\tau) - (1+2P)\frac{\partial W_1}{\partial Q} - \frac{\partial W_1}{\partial \tau} \end{aligned} \tag{5.13}$$

and

$$H_1(Q,P,\tau) = \frac{P}{\delta}\mathscr{G}_0(P)\cos\left(\frac{\omega}{\sqrt{\delta}}\tau\right) + \frac{P}{2\delta}\sum_{m=1}^{\infty}\mathscr{G}_m(P)\left[\cos\left(\frac{2mQ}{J'(P)} + \frac{\omega}{\sqrt{\delta}}\tau\right) + \cos\left(\frac{2mQ}{J'(P)} - \frac{\omega}{\sqrt{\delta}}\tau\right)\right]. \tag{5.14}$$

The phase space of the system defined by Eq. (5.14) contains an infinite number of resonance bands, each arising from a cosine term of the form

$$\cos\left(\frac{2mQ}{J'(P)} - \frac{\omega}{\sqrt{\delta}}\tau\right), \quad m = 1,2,3,\ldots\ .$$

By focusing our analysis on a single resonance band in (Q,P) space, i.e. by restricting P to a neighborhood of P_m — the location of the resonant torus in phase space associated with periodic orbits in $2m$:1 resonance with the parametric forcing — we can choose W_1 to eliminate all but one of the infinitely many terms of K_1. Thus, an appropriate choice for W_1 yields the following Kamiltonian valid in a neighborhood of P_m:

$$K(Q,P,\tau) = P + P^2 + \frac{\varepsilon}{2\delta}P\mathscr{G}_m(P)\cos\left(\frac{2mQ}{J'(P)} - \frac{\omega}{\sqrt{\delta}}\tau\right) + \mathcal{O}(\varepsilon^2). \tag{5.15}$$

The Lie generating function $W = W_1 + \mathcal{O}(\varepsilon)$ defining the corresponding canonical transformation is found to be

$$\begin{aligned} W_1(Q,P,\tau) = &\frac{P\mathscr{G}_0(P)}{\omega\sqrt{\delta}}\sin\left(\frac{\omega}{\sqrt{\delta}}\tau\right) \\ &+ \frac{P}{2\sqrt{\delta}}\sum_{n=1}^{\infty}{}'\mathscr{G}_n(P)\left[\frac{\sin(2nQ/J'(P) + (\omega/\sqrt{\delta})\tau)}{\omega + 2n\sqrt{\delta}\Omega(P)} - \frac{\sin(2nQ/J'(P) - (\omega/\sqrt{\delta})\tau)}{\omega - 2n\sqrt{\delta}\Omega(P)}\right], \end{aligned} \tag{5.16}$$

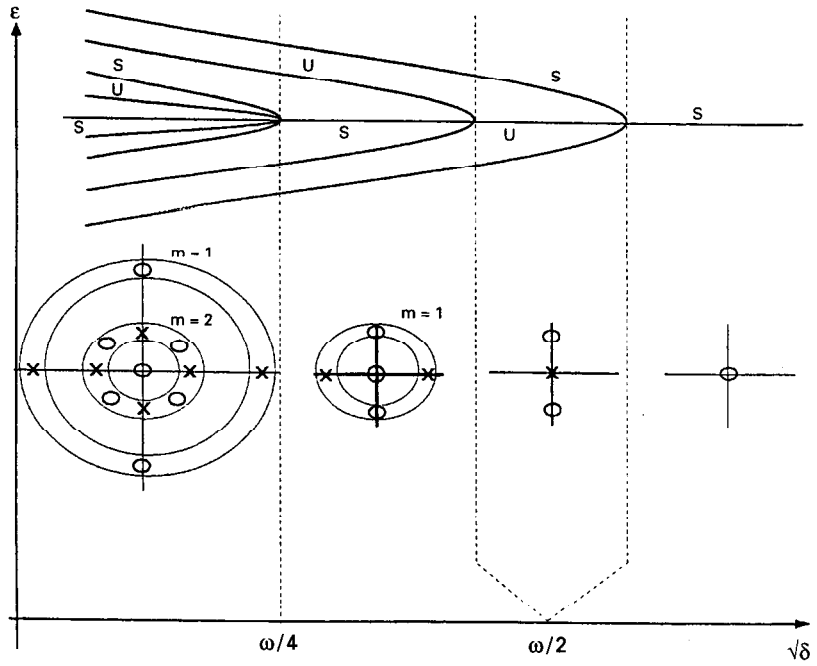

Fig. 3. Bifurcation of the 2 : 1 and 4 : 1 subharmonics in the non-linear Mathieu equation (emergence of resonance bands corresponding to $m = 1$ and 2). The $m = 2$ resonance band has a relative width much smaller than that implied by the illustration.

where we made the substitution, $\Omega(P) = (1 + 2P)/J'(P)$; the prime in the summation indicates that $n \neq m$. We see that resonant frequencies correspond to vanishing denominators of W_1.

The resonance relation $\omega/\sqrt{\delta} = 2m\Omega(P_m)$ also implies a condition for the "birth" and existence of resonance bands. Since $\Omega(P) \geqslant 1$ is an increasing function of $P \geqslant 0$, the resonant band associated with $2m:1$ subharmonic periodic motions is present precisely when

$$\frac{\omega}{\sqrt{\delta}} \geqslant 2m.$$

As the forcing frequency ω is increased for fixed δ, or as δ is decreased for fixed ω, resonant bands of higher order emerge from the origin and "propagate" away in phase space. The emergence of resonance bands at the origin can be seen as resulting from a series of pitchfork bifurcations. The above analysis as well as the results from Month and Rand [1] suggest that the quasistatic reduction of δ (keeping both ε and ω fixed) produces the bifurcation diagram shown in Fig. 3. In the general case, the $2m$ prongs of the pitchfork correspond to $2m:1$ subharmonic periodic motions of the non-linear Mathieu equation (1.1), while the handle corrsponds to the zero solution.

Finally, the time dependence in Kamiltonian (5.15) can be removed by making a canonical change of coordinates from (Q, P) to the "rest frame of reference" (ψ, Y) via the global generating function,

$$F(Q, Y, \tau) = QY - \frac{\omega}{2m\sqrt{\delta}} J(Y)\tau. \tag{5.17}$$

The transformation defined by (5.17) is given by

$$P = \frac{\partial F}{\partial Q}(Q, Y, \tau)$$
$$= Y \tag{5.18}$$

and

$$\psi = \frac{\partial F}{\partial Y}(Q, Y, \tau)$$
$$= Q - \frac{\omega}{2m\sqrt{\delta}} J'(Y)\tau,$$
$$= Q - \frac{\omega}{2m\sqrt{\delta}} J'(P)\tau. \tag{5.19}$$

The transformed Kamiltonian takes the form, up to $\mathcal{O}(\varepsilon^2)$,

$$K_r(\psi, Y) = K(Q, P) + \frac{\partial F}{\partial \tau}(Q, Y, \tau)$$
$$= Y + Y^2 - \frac{\omega}{2m\sqrt{\delta}} J(Y) + \frac{\varepsilon}{2\delta} Y \mathscr{G}_m(Y) \cos\left(\frac{2m\psi}{J'(Y)}\right). \tag{5.20}$$

In the new coordinate system, the transformed Kamiltonian $K_r(\psi, Y)$ does not depend explicitly on time and, therefore, remains constant. This means that the system is conservative and, hence, integrable. We shall refer to K_r as the *resonance Kamiltonian* since we can infer the dynamics of the original system only for action values near and within the resonance band associated with $2m:1$ subharmonic periodic orbits.

Transforming back to (x, y) coordinates, the level curves of K_r correspond to invariant curves of a Poincaré map induced by solutions of the non-linear Mathieu equation (1.1). For example, Fig. 4 presents the level curves of K_r in the ψ–Y plane for $m = 1$. The resonance band is bounded by action values, $Y \approx 1.4$ and 2.8, and possesses two centers and two saddle points. If transformed back to (x, y) coordinates, this band is mapped into the elliptical annulus centered at the origin in the x–y plane. The Poinaré map shown in Fig. 5 illustrates the predicted result of such a transformation. It was generated numerically whereby solutions of the non-linear Mathieu equation, obtained from the Dynamical System Toolkit "dstool" [11], are strobed at times $t_n = n2\pi/\omega$, $n = 1, 2, 3, \ldots$. In the next section, we derive analytic expressions for features of the resonance band — namely, location of equilibrium points and width of the resonance band — and "translate" these results in terms of the original (x, y) coordinates.

6. Structure of resonance bands in the non-linear Mathieu equation

In this section, we focus exclusively on the resonance band associated with periodic orbits in $2m:1$ resonance with the parametric forcing. The band emerges from an action value Y_m (location of the resonant torus in phase space) that is determined by the resonance relation

$$\frac{\omega}{\sqrt{\delta}} = 2m\Omega(Y_m). \tag{6.1}$$

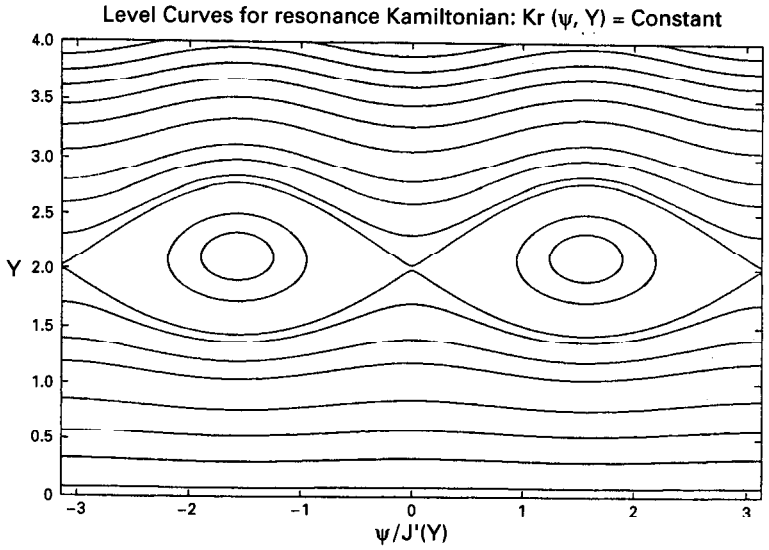

Fig. 4. Level curves of the resonant Kamiltonian, K_r, as seen in the ψ–Y plane. The resonance band is bounded by action values, $Y \approx 1.4$ and $Y \approx 2.8$.

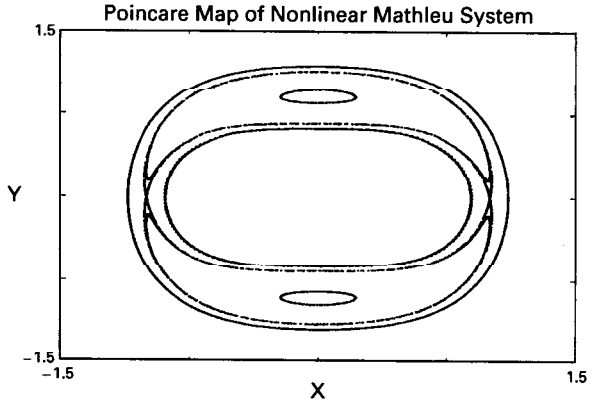

Fig. 5. Numerically generated Poincaré map induced by solutions of the non-linear Mathieu equation: $\delta = 0.25$, $\varepsilon = 0.05$, $\omega = 2.0$, and $\alpha = 1$. The solution is strobed at times $t_n = n2\pi/\omega$, $n = 1, 2, 3, \ldots$.

Using the resonance Kamiltonian, K_r, we obtain analytic expressions for the location of equilibrium points and the width of the resonance band. We do not examine the dynamics in the stochastic layers arising from the intersection of the invariant manifolds of saddle points, since the integrable nature of the unperturbed system is preserved under the perturbation method.

6.1. Location of equilibrium points

Consider the resonance band associated with periodic orbits in $2m$:1 resonance with the parametric forcing. The band emerges from a resonant torus — an invariant closed curve of the unperturbed Poincaré

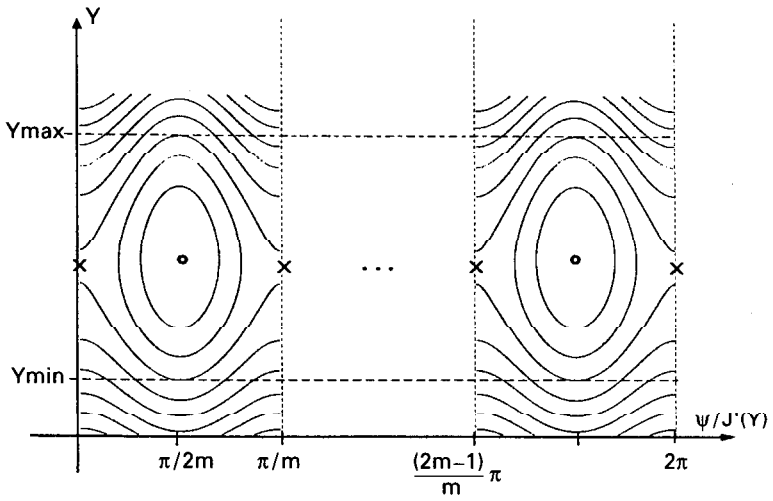

Fig. 6. Sketch of the level curves of the resonance Kamiltonian, K_r. The illustrated resonance band corresponds to a $2m:1$ resonance with the parametric forcing and is seen to have a topological structure consisting of a region bounded by a pair of heteroclinic motions, similar to that of a pendulum system (repeated $2m$ times). The band emerges from an action value Y_m as determined by the resonance relation, $\omega/\sqrt{\delta} = 2m\Omega(Y_m)$. The three dots represent $2m-2$ additional copies of the displayed phase portraits.

map — located in phase space at $Y = Y_m$ for which the resonance relation holds. As discussed in [6], the torus is filled with degenerate periodic points that split into $2m$ hyperbolic saddle points and $2m$ elliptic centers when the perturbation is introduced. The result in phase space is the resonance band illustrated in Fig. 6. We shall derive analytic expressions for the location of the aforementioned equilibrium points as functions of the parameter values, $(\delta, \varepsilon, \omega)$.

The vector field associated with the resonance Kamiltonian, K_r, is determined by Hamilton's equations[5] and found to be

$$Y' = -\frac{\partial Kr}{\partial \psi} = \frac{\varepsilon m}{\delta} \frac{Y\mathcal{G}_m(Y)}{J'(Y)} \sin\left(\frac{2m\psi}{J'(Y)}\right), \tag{6.2}$$

$$\psi' = \frac{\partial Kr}{\partial Y} = 1 + 2Y - \frac{\omega}{2m\sqrt{\delta}} J'(Y) + \frac{\varepsilon}{2\delta}\left[(Y\mathcal{G}_m(Y))' \cos\left(\frac{2m\psi}{J'(Y)}\right) + 2m\psi \frac{J''(Y)}{J'(Y)} Y\mathcal{G}_m(Y) \sin\left(\frac{2m\psi}{J'(Y)}\right)\right]. \tag{6.3}$$

The equilibrium points satisfy $Y' = 0$ and $\psi' = 0$, the former implying that either $Y = 0$, which corresponds to the origin, or

$$\sin\left(\frac{2m\psi}{J'(Y)}\right) = 0. \tag{6.4}$$

[5] Recall that the prime denotes differentiation with respect to τ, the scaled time.

Concerning ourselves with non-trivial solutions, the condition $\psi' = 0$ along with (6.4) asserts that the action values of equilibrium points are determined by solving the equation

$$1 + 2Y - \frac{\omega}{2m\sqrt{\delta}}\sqrt{1 + 2Y}\tilde{K}(Y) \pm \frac{\varepsilon}{2\delta}(Y\mathscr{G}_m(Y))' = 0. \tag{6.5}$$

Saddle points correspond to the " + " case (cosine = + 1) and centers correspond to the " − " case (cosine = − 1). For either case, their locations are perturbations of Y_m. That is, the action value for each saddle point has the form $Y_s = Y_m - \mathcal{O}(\varepsilon)$, and the action value for each center has the form $Y_c = Y_m + \mathcal{O}(\varepsilon)$. Indeed, to lowest order ($\varepsilon = 0$), Eq. (6.5) reduces to

$$1 + 2Y - \frac{\omega}{2m\sqrt{\delta}}\sqrt{1 + 2Y}\tilde{K}(Y) = 0$$

or equivalently,

$$\frac{\omega}{\sqrt{\delta}} = 2m\frac{\sqrt{1 + 2Y}}{\tilde{K}(Y)} - 2m\Omega(Y),$$

which is the resonance relation satisfied by $Y = Y_m$.

Determining analytic expressions for the location of saddle points and centers can be handled simultaneously. Assume that solutions Y_* to (6.5) have the form

$$Y_* = Y_m + \varepsilon\Delta Y + \mathcal{O}(\varepsilon^2). \tag{6.6}$$

Substituting Eq. (6.6) into (6.5), expanding the resulting expression in a Taylor series about $\varepsilon = 0$, and equating coefficients of like powers of ε to zero, we find that

$$\Delta Y = \mp\frac{1}{2\delta}\frac{\mathscr{G}_m(Y_m) + Y_m\mathscr{G}'_m(Y_m)}{1 - \Omega(Y_m)\sqrt{1 + 2Y_m}\tilde{K}'(Y_m)} \tag{6.7}$$

so that

$$Y_s = Y_m - \frac{\varepsilon}{2\delta}\frac{\mathscr{G}_m(Y_m) + Y_m\mathscr{G}'_m(Y_m)}{1 - \Omega(Y_m)\sqrt{1 + 2Y_m}\tilde{K}'(Y_m)} + \mathcal{O}(\varepsilon^2) \tag{6.8}$$

and

$$Y_c = Y_m + \frac{\varepsilon}{2\delta}\frac{\mathscr{G}_m(Y_m) + Y_m\mathscr{G}'_m(Y_m)}{1 - \Omega(Y_m)\sqrt{1 + 2Y_m}\tilde{K}'(Y_m)} + \mathcal{O}(\varepsilon^2). \tag{6.9}$$

The above expressions hold for all $m = 1, 2, 3, \ldots$. Referring to Eq. (4.15), $\mathscr{G}_1(Y) = \frac{1}{2} + \mathcal{O}(Y^2)$. We can, therefore, directly solve Eq. (6.5) for the location of the equilibrium points for the $m = 1$ case, rather than expanding the solution in a power series in ε. Substituting $\mathscr{G}_1(Y) = \frac{1}{2}$ into Eq. (6.5) and approximating [6] $\tilde{K}(Y_*) \approx \tilde{K}(Y_1)$ so that

$$\frac{\omega}{2\sqrt{\delta}}\tilde{K}(Y_*) \approx \frac{\omega}{2\sqrt{\delta}}\tilde{K}(Y_1) = \sqrt{1 + 2Y_1} = r_0,$$

[6] The function $\tilde{K}(Y)$ is a slowly varying, increasing function of Y and assumes values only in the interval $[1, 1.1804]$.

Eq. (6.5) reduces to the following quadratic equation for $r_* = \sqrt{1 + 2Y_*}$:

$$r_*^2 - \frac{\omega}{2\sqrt{\delta}}\tilde{K}(Y_1)r_* \pm \frac{\varepsilon}{4\delta} = r_*^2 - r_0 r_* \pm \frac{\varepsilon}{4\delta} = 0. \tag{6.10}$$

Solving, the one viable root ($r_* \geqslant 1$) is found to be

$$r_* = \frac{1}{2}\left[r_0 + \sqrt{r_0^2 \mp \frac{\varepsilon}{\delta}}\right] \tag{6.11}$$

and it follows that

$$Y_* = \frac{1}{4}\left[r_0^2 + \sqrt{r_0^2 \mp \frac{\varepsilon}{\delta}} - 2\right] \mp \frac{\varepsilon}{8\delta}. \tag{6.12}$$

Here the upper sign refers to the saddle, and the lower sign refers to the center.

6.2. *Width of resonance band in action space*

As illustrated in Fig. 6, the resonance band occupies a finite region of phase space bounded by a pendulum-like separatrix. Moreover, the resonance band emerges from a resonant torus at an action value satisfying the resonance relation,

$$\frac{\omega}{\sqrt{\delta}} = 2m\Omega(Y_m).$$

Although the phase space of the unperturbed system becomes greatly distorted in the vicinity of the resonance band when the perturbation is introduced, trajectories outside the separatrix behave almost as if the system is not perturbed. Therefore, it is of interest to determine the extent of the resonance band. We shall show that the width of the resonance band is of order $\sqrt{Y_m \mathscr{G}_m(Y_m)\varepsilon/\delta}$, and we shall derive analytic expressions for $Y_{\min}$ and $Y_{\max}$, the minimum and maximum action values acquired by the bounding separatrix, respectively.

The separatrix is the level curve of the resonance Kamiltonian that passes through saddle points. The value of the resonance Kamiltonian on the separatrix is, therefore

$$K_r\left(\cos\left(\frac{2m\psi}{J'(Y_s)}\right) = 1,\ Y = Y_s\right) = Y_s + Y_s^2 - \frac{\omega}{2m\sqrt{\delta}}J(Y_s) + \frac{\varepsilon}{2\delta}Y_s\mathscr{G}_m(Y_s), \tag{6.13}$$

where Y_s is the action value of the saddle points of the resonance band. The maximum extent of the resonance band occurs when $\cos(2m\psi/J'(Y)) = -1$, the same phase for centers, and the resonance Kamiltonian for this phase takes the form

$$K_r\left(\cos\left(\frac{2m\psi}{J'(Y_s)}\right) = -1, Y\right) = Y + Y^2 - \frac{\omega}{2m\sqrt{\delta}}J(Y) - \frac{\varepsilon}{2\delta}Y\mathscr{G}_m(Y). \tag{6.14}$$

Equating Eqs. (6.13) and (6.14), we obtain the following equation in Y for $Y_{\min}$ and $Y_{\max}$:

$$(Y - Y_s) + (Y^2 - Y_s^2) - \frac{\omega}{2m\sqrt{\delta}}(J(Y) - J(Y_s)) - \frac{\varepsilon}{2\delta}(Y\mathscr{G}_m(Y) + Y_s\mathscr{G}_m(Y_s)) = 0. \tag{6.15}$$

Analytic expressions for $Y_{\min}$ and $Y_{\max}$ are derived simultaneously. Assume that solutions $Y = Y_*$ to Eq. (6.15) are perturbations of Y_m of the form

$$Y_* = Y_m + W\varepsilon^\alpha + \mathcal{O}(\varepsilon^{2\alpha}) \tag{6.16}$$

and use Eq. (6.8) for Y_s, $Y_s = Y_m - \Delta Y\varepsilon + \mathcal{O}(\varepsilon^2)$. Substituting Eqs. (6.8) and (6.16) into Eq. (6.15) and expanding the resulting expression in a Taylor series about $\varepsilon = 0$, we obtain consistent results only if $\alpha = \frac{1}{2}$. Moreover, by equating like coefficients of powers of ε to zero, we find

$$W^2 = \frac{Y_m\mathscr{G}_m(Y_m)}{\delta(1 - (\omega/4m\sqrt{\delta})J''(Y_m))}, \tag{6.17}$$

so that

$$Y_{\min} = Y_m - \sqrt{\frac{Y_m\mathscr{G}_m(Y_m)}{\delta(1 - (\omega/4m\sqrt{\delta})J''(Y_m))}}\varepsilon + \mathcal{O}(\varepsilon) \tag{6.18}$$

and

$$Y_{\max} = Y_m + \sqrt{\frac{Y_m\mathscr{G}_m(Y_m)}{\delta(1 - (\omega/4m\sqrt{\delta})J''(Y_m))}}\varepsilon + \mathcal{O}(\varepsilon). \tag{6.19}$$

We see that the width of the resonance band associated with subharmonic periodic orbits in $2m:1$ resonance with the parametric forcing is of order $\sqrt{Y_m\mathscr{G}_m(Y_m)\varepsilon/\delta}$. Referring to Eqs. (4.14) and (4.15), the functions $\mathscr{G}_m$ decrease roughly exponentially with increasing m. We see, therefore, that the $m = 1$ and 2 bands are most prominent for small ε.

7. Numerical integration and comparison with theory

In the preceding sections, we presented an $\mathcal{O}(\varepsilon)$ perturbation method to investigate the nature of subharmonic resonances in the non-linear Mathieu equation

$$\ddot{x} + (\delta + \varepsilon\cos\omega t)x + \alpha x^3 = 0.$$

The methodology involved the construction of the resonance Kamiltonian, K_r, explicit knowledge of which enabled us to derive analytic expressions for features of resonance bands in a Poincaré section of (ψ, Y)-space associated with $2m:1$ subharmonic periodic solutions. The purpose of this section is to demonstrate the accuracy of this perturbation method by comparing its results to those generated from the direct numerical integration of Eq. (1.1) using dstool.

The $2m$ hyperbolic saddle points and the $2m$ elliptic centers of the resonance band, singular points of the vector field associated with K_r, correspond to $2m:1$ subharmonic periodic solutions of the non-linear Mathieu equation (1.1). Their existence can be experimentally ascertained by numerically generating Poincaré maps whereby solutions are strobed at times $t_n = n2\pi/\omega$, $n = 1, 2, 3, \ldots$. Since the resonance band

occupies a finite region of phase space corresponding to an elliptical annulus centered at the origin in the $(x, \dot{x})$ phase plane (cf. Figs. 4 and 5), it is generally difficult to locate the above-mentioned equilibrium points of the numerically generated Poincaré map. In fact, it is not uncommon when performing numerical experiments to inadvertently miss the smaller (large m) zones of resonance. Therefore, the analytic techniques for locating the resonance band and associated equilibrium points in (ψ, Y)-space, in conjunction with the transformation $(\psi, Y) \to (x, \dot{x})$ back to the original coordinates, can be quite useful to this end.

Recall the following results pertaining to the resonance band in (ψ, Y)-space associated with $2m:1$ subharmonic periodic motions:

1. The action value $Y = Y_m$ of the resonant torus from which the resonance band emerges satisfies the resonance relation given by Eq. (6.1):

$$\frac{\omega}{\sqrt{\delta}} = 2m\Omega(Y_m).$$

2. The action values of equilibrium points, saddles (+) and centers (−), satisfy Eq. (6.5):

$$1 + 2Y - \frac{\omega}{2m\sqrt{\delta}}\sqrt{1 + 2Y}\tilde{K}(Y) \pm \frac{\varepsilon}{2\delta}(Y\mathcal{G}_m(Y))' = 0.$$

In addition, the corresponding phase ψ_s of the saddle point satisfies

$$\cos\left(\frac{2m\psi_s}{J'(Y_s)}\right) = 1$$

and the corresponding phase ψ_c of the center satisfies

$$\cos\left(\frac{2m\psi_c}{J'(Y_c)}\right) = -1,$$

where $Y = Y_s$ and $Y = Y_c$ are the action values for saddle points and centers, respectively.

3. The minimum and maximum action values, $Y = Y_{\min}$ and $Y = Y_{\max}$, acquired by the bounding separatrix satisfy Eq. (6.15):

$$(Y - Y_s) + (Y^2 - Y_s^2) - \frac{\omega}{2m\sqrt{\delta}}(J(Y) - J(Y_s)) - \frac{\varepsilon}{2\delta}(Y\mathcal{G}_m(Y) + Y_s\mathcal{G}_m(Y_s)) = 0.$$

In order to utilize these results, we must transform the (ψ, Y) coordinates back to the original, unscaled $(x, \dot{x})$ coordinates. To lowest order in ε, the transformation

$$Y \to P \to j$$

is near identity:

$$Y = j + \mathcal{O}(\varepsilon).$$

Furthermore, the action j satisfies

$$j = \tfrac{1}{2}X_i^2, \tag{7.1}$$

$$H_0 = h(j) = j + j^2 = \tfrac{1}{2}y^2 + \tfrac{1}{2}X^2 + \tfrac{1}{4}X^4, \tag{7.2}$$

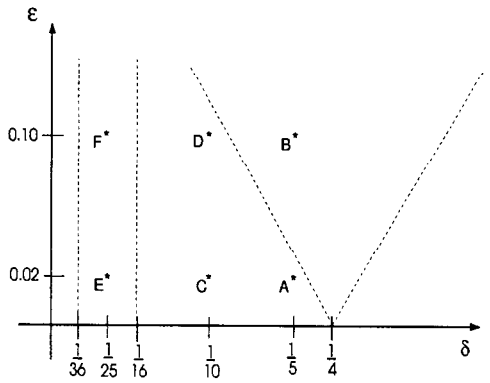

Fig. 7. Parameter values used to test the accuracy of the perturbation analysis. The dashed lines correspond to parameter values in the $\varepsilon - \delta$ parameter plane at which higher-order resonance bands emerge from the origin (i.e. bifurcation of 2:1 and 4:1 subharmonics in the non-linear Mathieu equation). Refer to the bifurcation diagram of Fig. 3.

where $(X, y = \mathrm{d}X/\mathrm{d}\tau)$ are the coordinates of the scaled system. Therefore, if the phase ψ corresponds to points for which $X = \pm X_t$ (as is the case for saddle points when $m = 1$), the associated X-value is obtained from Eq. (7.1):

$$X = \pm X_t = \pm\sqrt{2j} = \pm\sqrt{2Y}. \tag{7.3}$$

Or, if the phase ψ corresponds to points for which $X = 0$, (as is the case for centers when $m = 1$), the associated y-value is obtained from Eq. (7.2):

$$y = \pm\sqrt{2H_0} = \pm\sqrt{2(j + j^2)} = \pm\sqrt{2(Y + Y^2)}. \tag{7.4}$$

Finally, the scaled (X, y) coordinates are transformed back to the original, unscaled $(x, \dot{x})$ coordinates via the relations (cf. Section 3):

$$x = \sqrt{\frac{\delta}{\alpha}}X,$$

$$\dot{x} = \frac{\mathrm{d}x}{\mathrm{d}t} = \frac{\mathrm{d}x}{\mathrm{d}X}\frac{\mathrm{d}X}{\mathrm{d}\tau}\frac{\mathrm{d}\tau}{\mathrm{d}t} = \sqrt{\frac{\delta}{\alpha}}\cdot y\cdot\sqrt{\delta} = \frac{\delta}{\sqrt{\alpha}}y.$$

In the remainder of this section, we present quantitative predictions for features of the resonance band in the $(x, \dot{x})$ phase space for the parameter values indicated in Fig. 7. We predict the location of equilibrium points in the resonance band as well as its width, as derived from the perturbation analysis along with the aforementioned transformation $(\psi, Y) \to (x, \dot{x})$, and compare these results to those generated from the direct numerical integration of Eq. (1.1) using dstool. Specifically, Poincaré maps for the non-linear Mathieu equation are numerically generated, and quantitative information pertaining to the resonance bands is extracted directly from them. A summary of the comparison of the results for each parameter value is given below. Without loss of generality, we set $\omega = 1$ and $\alpha = 1$; only the parameters δ and ε are varied.

	Predicted Value	Actual Value	Absolute Error
Saddle Points			
x-coordinate	$\pm$ 0.233	$\pm$ 0.2320	0.0010
$\dot{x}$-coordinate	0.000	0.0000	0.0000
Centers			
x-coordinate	0.000	0.0000	0.0000
$\dot{x}$-coordinate	$\pm$ 0.138	$\pm$ 0.1390	0.0010
Outer Separatrix			
x-coordinate	0.000	0.0000	0.0000
$\dot{x}$-coordinate	$\pm$ 0.191	0.1916	0.0006
Inner Separatrix			
x-coordinate	0.000	0.0000	0.0000
$\dot{x}$-coordinate	$\pm$ 0.066	0.0664	0.0004

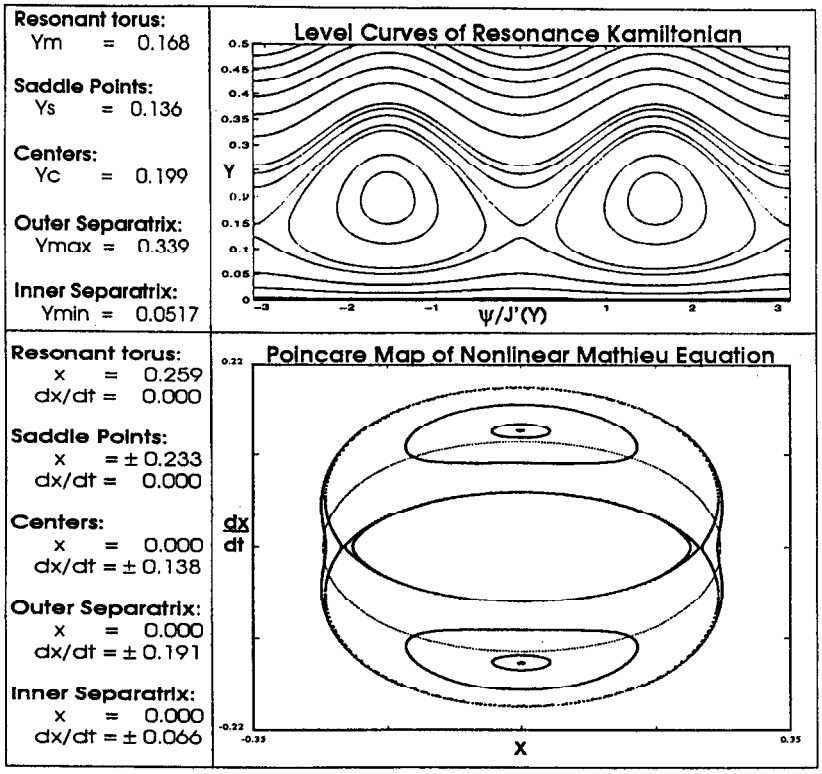

Fig. 8. Level curves of the resonance Kamiltonian, K_r, and numerically generated Poincaré map for the non-linear Mathieu equation (1.1). The parameter values associated with this figure correspond to point A: $\delta = 0.20$, $\varepsilon = 0.02$, $\omega = 1$, and $\alpha = 1$. The action values Y for various features of the resonance band in (ψ, Y) coordinates are obtained from the perturbation method and are used to compute estimates for the $(x,\dot{x})$-coordinates of the corresponding features. The small, dotted line represents the resonant torus of the unperturbed system from which the resonance band emerges.

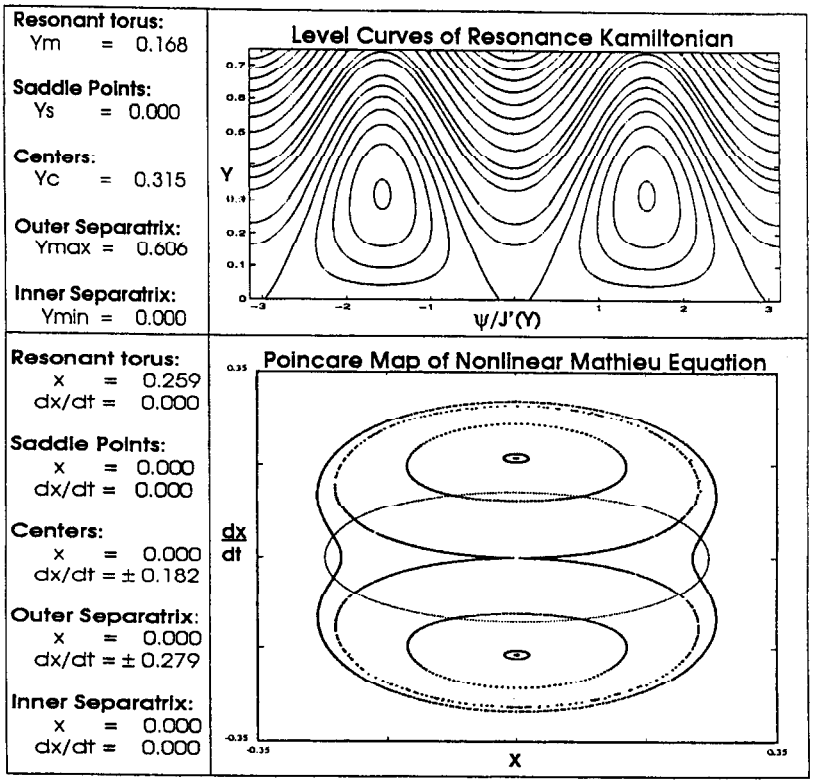

Fig. 9. Level curves of the resonance Kamiltonian, K_r, and numerically generated Poincaré map for the non-linear Mathieu equation (1.1). The parameter values associated with this figure correspond to point B: $\delta = 0.20$, $\varepsilon = 0.10$, $\omega = 1$, and $\alpha = 1$. The action values Y for various features of the resonance band in (ψ, Y) coordinates are obtained from the perturbation method and are used to compute estimates for the $(x,\dot{x})$-coordinates of the corresponding features. The small, dotted line represents the resonant torus of the unperturbed system from which the resonance band emerges. Notice that the origin is an unstable saddle for these parameter values.

	Predicted Value	Actual Value	Absolute Error
Saddle Points			
x-coordinate	0.000	0.0000	0.0000
$\dot{x}$-coordinate	0.000	0.0000	0.0000
Centers			
x-coordinate	0.000	0.0000	0.0000
$\dot{x}$-coordinate	$\pm$ 0.182	$\pm$ 0.1878	0.0058
Outer Separatrix			
x-coordinate	0.000	0.0000	0.0000
$\dot{x}$-coordinate	$\pm$ 0.279	0.2867	0.0077
Inner Separatrix			
x-coordinate	0.000	0.0000	0.0000
$\dot{x}$-coordinate	0.000	0.0000	0.0000

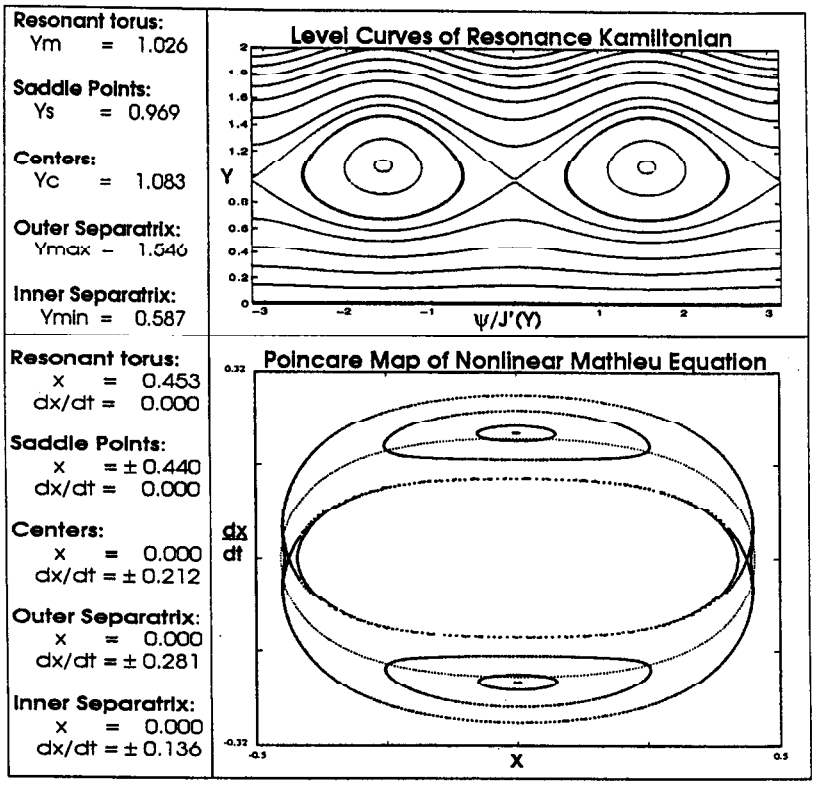

Fig. 10. Level curves of the resonance Kamiltonian, K_r, and numerically generated Poincaré map for the non-linear Mathieu equation (1.1). The parameter values associated with this figure correspond to point C: $\delta = 0.10$, $\varepsilon = 0.02$, $\omega = 1$, and $\alpha = 1$. The action values Y for various features of the resonance band in (ψ, Y) coordinates are obtained from the perturbation method and are used to compute estimates for the $(x,\dot{x})$-coordinates of the corresponding features. The small, dotted line represents the resonant torus of the unperturbed system from which the resonance band emerges.

	Predicted Value	Actual Value	Absolute Error
Saddle Points			
x-coordinate	± 0.440	± 0.4377	0.0023
$\dot{x}$-coordinate	0.000	0.0000	0.0000
Centers			
x-coordinate	0.000	0.0000	0.0000
$\dot{x}$-coordinate	± 0.212	± 0.2133	0.0013
Outer Separatrix			
x-coordinate	0.000	0.0000	0.0000
$\dot{x}$-coordinate	± 0.281	± 0.2816	0.0006
Inner Separatrix			
x-coordinate	0.000	0.0000	0.0000
$\dot{x}$-coordinate	± 0.136	± 0.1373	0.0013

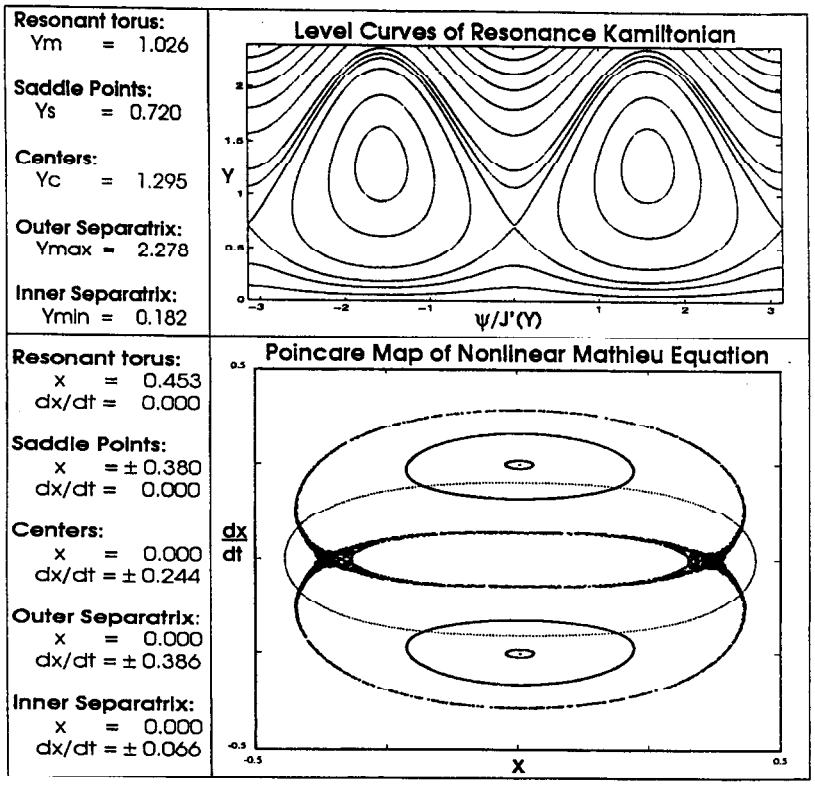

Fig. 11. Level curves of the resonance Kamiltonian, K_r, and numerically generated Poincaré map for the non-linear Mathieu equation (1.1). The parameter values associated with this figure correspond to point D: $\delta = 0.10$, $\varepsilon = 0.10$, $\omega = 1$, and $\alpha = 1$. The action values Y for various features of the resonance band in (ψ, Y) coordinates are obtained from the perturbation method and are used to compute estimates for the $(x,\dot{x})$-coordinates of the corresponding features. The small, dotted line represents the resonant torus of the unperturbed system from which the resonance band emerges.

	Predicted Value	Actual Value
Saddle Points		
x-coordinate	± 0.380	$\pm [0.350, 0.390]$
$\dot{x}$-coordinate	0.000	0.000
Centers		
x-coordinate	0.000	0.0000
$\dot{x}$-coordinate	± 0.244	± 0.2504
Outer Separatrix		
x-coordinate	0.000	0.0000
$\dot{x}$-coordinate	± 0.386	$\pm [0.3938, 0.3952]$
Inner Separatrix		
x-coordinate	0.000	0.0000
$\dot{x}$-coordinate	± 0.066	$\pm [0.0687, 0.0709]$

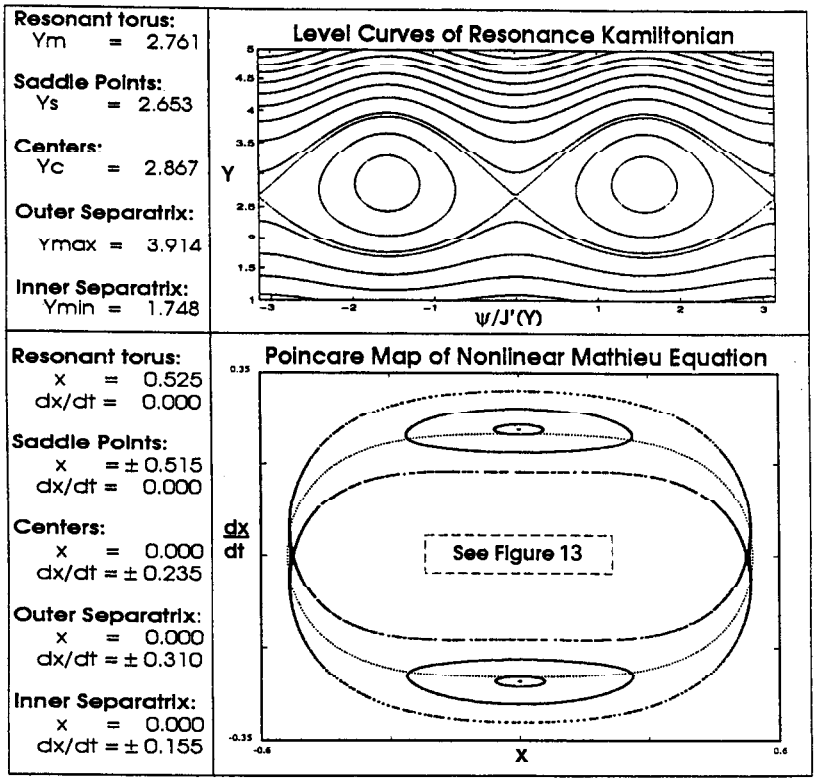

Fig. 12. Level curves of the resonance Kamiltonian, K_r, and numerically generated Poincaré map for the non-linear Mathieu equation (1.1). The parameter values associated with this figure correspond to point E: $\delta = 0.05$, $\varepsilon = 0.02$, $\omega = 1$, and $\alpha = 1$. The action values Y for various features of the resonance band in (ψ, Y) coordinates are obtained from the perturbation method and are used to compute estimates for the $(x,\dot{x})$-coordinates of the corresponding features. The small, dotted line represents the resonant torus of the unperturbed system from which the resonance band emerges.

	Predicted Value	Actual Value	Absolute Error
Saddle Points			
x-coordinate	± 0.515	± 0.5121	0.0029
$\dot{x}$-coordinate	0.000	0.0000	0.0000
Centers			
x-coordinate	0.000	0.0000	0.0000
$\dot{x}$-coordinate	± 0.235	± 0.2364	0.0014
Outer Separatrix			
x-coordinate	0.000	0.0000	0.0000
$\dot{x}$-coordinate	± 0.310	± 0.3111	0.0011
Inner Separatrix			
x-coordinate	0.000	0.0000	0.0000
$\dot{x}$-coordinate	± 0.155	± 0.1561	0.0011

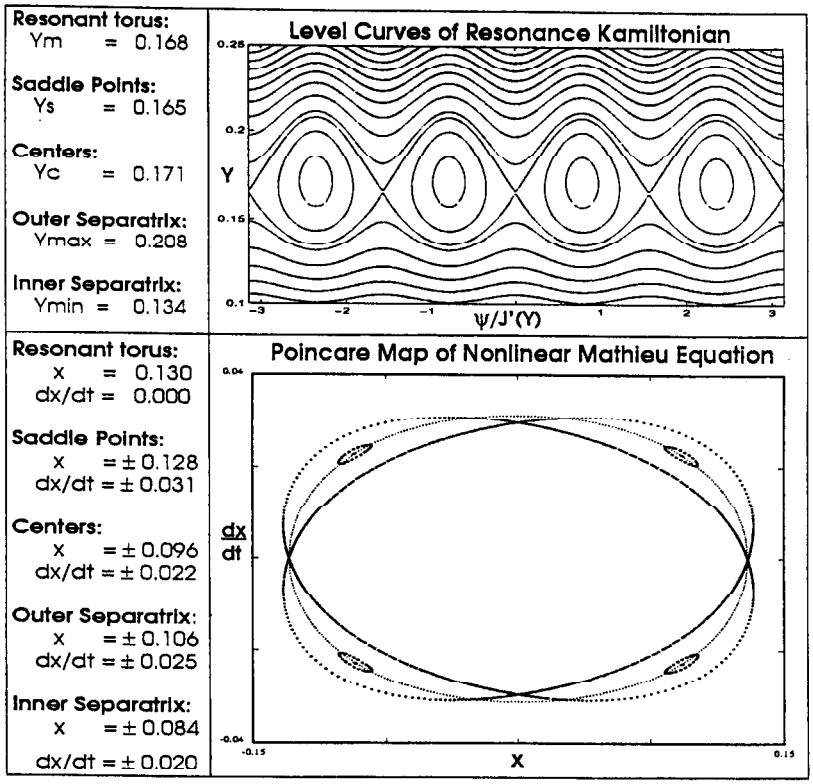

Fig. 13. Level curves of the resonance Kamiltonian, K_r, and numerically generated Poincaré map for the non-linear Mathieu equation (1.1). The parameter values associated with this figure correspond to point E: $\delta = 0.05$, $\varepsilon = 0.02$, $\omega = 1$, and $\alpha = 1$. The action values Y for various features of the resonance band in (ψ, Y) coordinates are obtained from the perturbation method and are used to compute estimates for the $(x, \dot{x})$-coordinates of the corresponding features. The small, dotted line represents the resonant torus of the unperturbed system from which the resonance band emerges.

	Predicted Value	Actual Value	Absolute Error
Saddle Points			
x-coordinate	$\pm$ 0.128	$\pm$ 0.1298	0.0018
$\dot{x}$-coordinate	$\pm$ 0.031	$\pm$ 0.0298	0.0012
Centers			
x-coordinate	$\pm$ 0.096	$\pm$ 0.0929	0.0031
$\dot{x}$-coordinate	$\pm$ 0.022	$\pm$ 0.0227	0.0007
Outer Separatrix			
x-coordinate	$\pm$ 0.106	$\pm$ 0.112	0.006
$\dot{x}$-coordinate	$\pm$ 0.025	$\pm$ 0.023	0.002
Inner Separatrix			
x-coordinate	$\pm$ 0.084	$\pm$ 0.081	0.003
$\dot{x}$-coordinate	$\pm$ 0.020	$\pm$ 0.020	0.000

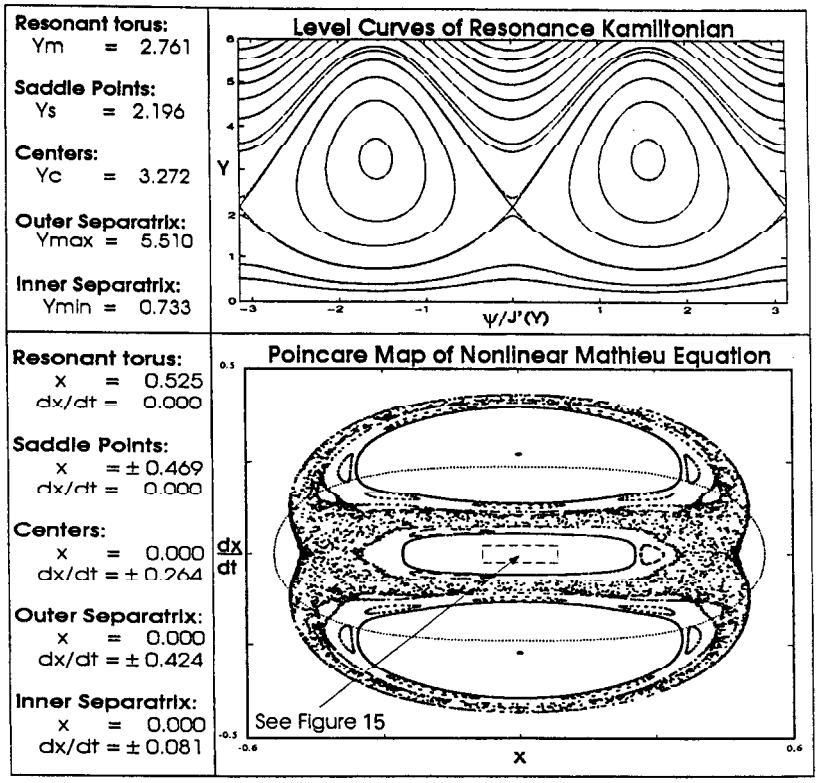

Fig. 14. Level curves of the resonance Kamiltonian, K_r, and numerically generated Poincaré map for the non-linear Mathieu equation (1.1). The parameter values associated with this figure correspond to point F: $\delta = 0.05$, $\varepsilon = 0.10$, $\omega = 1$, and $\alpha = 1$. The action values Y for various features of the resonance band in (ψ, Y) coordinates are obtained from the perturbation method and are used to compute estimates for the $(x,\dot{x})$-coordinates of the corresponding features. The small, dotted line represents the resonant torus of the unperturbed system from which the resonance band emerges.

	Predicted Value	Actual Value
Saddle Points		
x-coordinate	± 0.469	$\pm [0.349, 0.477]$
$\dot{x}$-coordinate	0.000	0.000
Centers		
x-coordinate	0.000	0.000
$\dot{x}$-coordinate	± 0.264	± 0.270
Outer Separatrix		
x-coordinate	0.000	0.000
$\dot{x}$-coordinate	± 0.424	$\pm [0.392, 0.432]$
Inner Separatrix		
x-coordinate	0.000	0.000
$\dot{x}$-coordinate	± 0.080	$\pm [0.069, 0.133]$

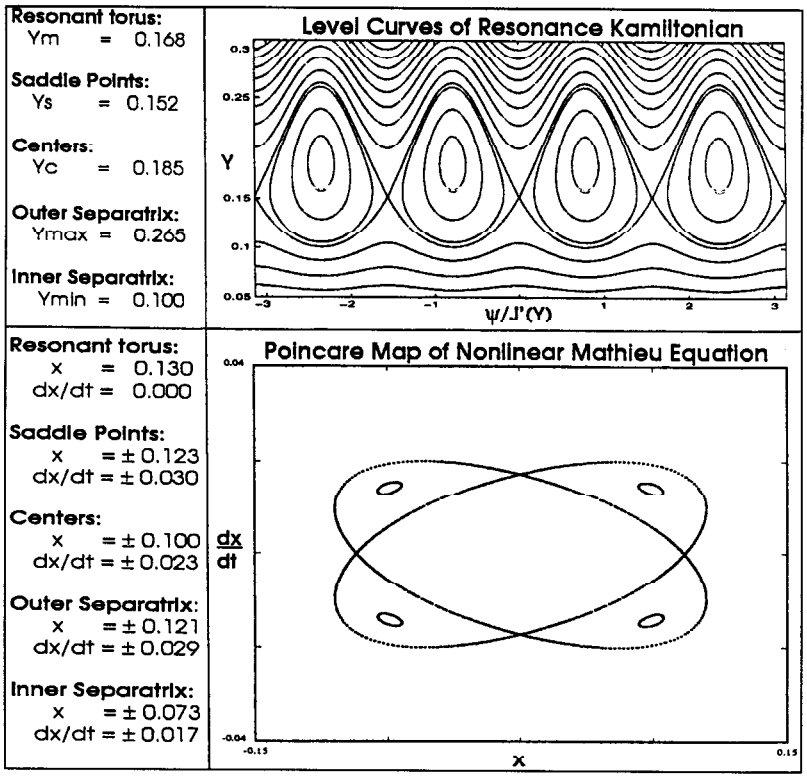

Fig. 15. Level curves of the resonance Kamiltonian, K_r, and numerically generated Poincaré map for the non-linear Mathieu equation (1.1). The parameter values associated with this figure correspond to point F: $\delta = 0.05$, $\varepsilon = 0.10$, $\omega = 1$, and $\alpha = 1$. The action values Y for various features of the resonance band in (ψ, Y) coordinates are obtained from the perturbation method and are used to compute estimates for the $(x,\dot{x})$-coordinates of the corresponding features.

	Predicted Value	Actual Value	Absolute Error
Saddle Points			
x-coordinate	$\pm$ 0.1233	$\pm$ 0.0929	0.0304
$\dot{x}$-coordinate	$\pm$ 0.0296	$\pm$ 0.0172	0.0124
Centers			
x-coordinate	$\pm$ 0.0998	$\pm$ 0.0746	0.0252
$\dot{x}$-coordinate	$\pm$ 0.0234	$\pm$ 0.0143	0.0091
Outer Separatrix			
x-coordinate	$\pm$ 0.121	$\pm$ 0.089	0.032
$\dot{x}$-coordinate	$\pm$ 0.029	$\pm$ 0.017	0.012
Inner Separatrix			
x-coordinate	$\pm$ 0.0725	$\pm$ 0.0560	0.0165
$\dot{x}$-coordinate	$\pm$ 0.0166	$\pm$ 0.0096	0.0070

It is worthwhile to remark that parameter points A, B, C, and D lead to only one resonance band in phase space, that associated with 2:1 subharmonic periodic orbits — i.e. the condition for the existence of $2m$:1 resonance bands, $\omega/\sqrt{\delta} \geqslant 2m$, holds for only $m = 1$. However, the $m = 2$ resonance

band associated with 4:1 subharmonic periodic orbits is present for parameter points E and F — i.e. the condition for the existence of $2m$:1 resonance bands holds for both $m = 1$ and 2. Refer to the bifurcation diagram of Fig. 3.

8. Conclusion

Previous studies [1,2] of the non-linear Mathieu equation

$$\ddot{x} + (\delta + \varepsilon\cos\omega t)x + \alpha x^3 = 0$$

have made use of perturbation schemes that begin with the simple harmonic oscillator the *linear*, unperturbed system — and involve the manipulation of trigonometric functions. Results obtained by these methods were necessarily restricted to the neighborhood of the origin and picked up only the 2:1 subharmonic at the $\mathcal{O}(\varepsilon)$ level of analysis. In contrast to these methods, the present study employed a perturbation scheme that perturbed off the *non-linear* oscillator,

$$\ddot{x} + \delta x + \alpha x^3 = 0$$

and the ensuing analysis necessitated the use of the elliptic functions $\mathrm{cn}(u,k)$, $\mathrm{sn}(u,k)$, and $\mathrm{dn}(u,k)$ instead of the trigonometric functions cosine and sine. This had the principal advantage that subharmonic resonances of all orders are picked up, even at the lowest order of perturbation analysis, $\mathcal{O}(\varepsilon)$, whereas in the trigonometric analysis one needs to go to $\mathcal{O}(\varepsilon^m)$ in order to pick up the $2m$:1 subharmonics (cf. [7]).

Using this technique, we were able to obtain approximate analytical expressions for the location and width of the regions in phase space corresponding to a $2m$:1 subharmonic resonance, for arbitrary integer m. As a demonstration and check of the validity of the approximations, we compared the predictions of the theory with those from the direct numerical integration of Eq. (1.1) for $m = 1$ and 2. These comparisons, which are presented in Figs. 8–15 for the parameters displayed in Fig. 7, show that the perturbation results are quite accurate, with smaller values of ε delivering expectedly better results than for larger values ($\varepsilon = 0.02$ versus $\varepsilon = 0.10$). Figs. 8–15 also demonstrate the inability of this perturbation method to show chaos (e.g. Fig. 14). Here the integrable nature of the unperturbed equation is preserved under the perturbation process. This is in contrast to, for example, Melnikov's method [6,10], which predicts the appearance of chaos by perturbing off of a homoclinic orbit (i.e. a saddle connection).

References

[1] L. Month, R. Rand, Bifurcation of 4:1 subharmonics in the non-linear Mathieu equation, Mech. Res. Commun. 9 (1982) 233–240.
[2] A.H. Nayfeh, D.T. Mook, Nonlinear Oscillations, Wiley, New York, 1979.
[3] S. Wiggins, Introduction to Applied Non-linear Dynamical Systems and Chaos, Springer, New York, 1990.
[4] R. Zounes, An analysis of the non-linear quasiperiodic Mathieu equation, Ph.D. Dissertation, Center for Applied Mathematics, Cornell University, Ithaca, NY, May 1997.
[5] S. Wiggins, Global Bifurcations and Chaos: Analytical Methods, Springer, New York, 1988.
[6] J. Guckenheimer, P. Holmes, Nonlinear Oscillations, Dynamical Systems, and Bifurcation of Vector Fields, Springer, New York, 1983.
[7] P.F. Byrd, M.D. Friedman, Handbook of Elliptic Integrals for Scientists and Engineers, Springer, New York, 1971.
[8] J.R. Cary, Lie transform perturbation theory for Hamiltonian systems, Phys. Rep. (Review section of Physics Lett.) 79 (1981) 129–159.
[9] A. Deprit, Canonical transformations depending on a parameter, Celestial Mech. 1 (1969) 1–31.
[10] R.H. Rand, Topics in Non-linear Dynamics with Computer Algebra, Gordon and Breach Science Publishers, Langhorne, Pennsylvania, 1994.
[11] J. Guckenheimer, M. Myers, F. Wicklin, P. Worfolk, dstool: a dynamical system toolkit with an interactive graphical interface, Department of Applied Mathematics, Cornell University, Ithaca, New York, 1991.